

ANALYSIS OF MICROPHONIC NOISE GENESIS AND MITIGATION IN A  
BORON CARBIDE DETECTOR SYSTEM

A Thesis

by

WILLIAM JAMES GORDON

Submitted to the Office of Graduate and Professional Studies of  
Texas A&M University  
in partial fulfillment of the requirements for the degree of

MASTER OF SCIENCE

Chair of Committee,	Leslie Braby
Committee Members,	Sunil Khatri
	Delia Perez-Nunez
Head of Department,	Yassin Hassan

August 2015

Major Subject: Health Physics

Copyright 2015 William James Gordon

## ABSTRACT

Boron lined ion chambers designed to monitor thermal flux between the fuel rods of a TRIGA Mark II pool type reactor were found to have excessive electronic and microphonic noise which overwhelmed the neutron signal in preliminary measurements. In order to effectively evaluate the detectors sensitivity to electrical and microphonic noise, a testing apparatus was constructed to provide consistent and reproducible geometry and decibel sound levels from test equipment. After careful testing, it was found that the main microphonic susceptibility was because of the triboelectric effect within the coaxial cable. This was eliminated with the use of a low-noise cable. Once the electronic noise was minimized and new cables were installed, an improved neutron measurement was made.

## DEDICATION

This thesis is dedicated to the teachers, musicians, artists who impact the world in profound ways.

## ACKNOWLEDGEMENTS

No achievement is ever obtained in isolation. Without the support of my advisors, Dr. Leslie Braby, Dr. Delia Perez-Nunez, and Dr. Sunil Khatri I would not have been able to succeed in graduate school. Dr. Khatri's insight and perspective into electric systems helped keep me focused on the problems at hand. Dr. Perez has always been a supportive mentor who showed me more opportunities than I knew existed while at Texas A&M, and encouraged me to pursue higher education at a critical juncture in life. Dr. Braby's meticulous analysis of experimental problems showed me an entirely new paradigm on concise troubleshooting and experimental design.

I would also like to thank Dr. Sean McDeavitt of the Fuel Cycle Materials Laboratory who provided my first work experiences in a large scale laboratory. The Nuclear Science Center at Texas A&M, especially Viktor Vlassov, provided exceptional help and resources.

John Vilas of Vilas Motor Works provided critical assistance when a component broke, for which I will always be grateful. Steve Scanlon's, who programmed ToneGen, work was appreciated and used extensively in testing the microphonic sensitivity of detector examined in this thesis. To my friends Jimmy Uhlemeyer and Timothy Jacomb-Hood who reviewed this thesis and offered suggestions. I would also like to acknowledge two great role models in my life, Mr. Dave Enos and Mr. Terence Schraut of Boy Scout Troop 61 in Los Fresnos Texas. They taught me what it means to live with integrity and how to be prepared for life challenges.

Finally I would like to thank my parents, sisters, and my brilliant fiancée Natalie Galegar for their love.

## NOMENCLATURE

DAQ	Data Acquisition System
DOE	Department of Energy
LET	Linear Energy Transfer
MCA	Multi-Channel Analyzer
MDPH	Minimum Detectable Pulse Height
MSM	Mean Square Voltage
NIM	Nuclear Instrumentation Module
NSC	Nuclear Science Center
PNNL	Pacific Northwest National Laboratory
RMS	Root Mean Square
STP	Standard Temperature and Pressure (20 °C, 1 atm)
TRIGA	Training Research Isotopes General Atomics
SCA	Single Channel Analyzer
SRIM	Stopping and Range of Ions in Matter

## TABLE OF CONTENTS

	Page
ABSTRACT .....	ii
DEDICATION .....	iii
ACKNOWLEDGEMENTS .....	iv
NOMENCLATURE .....	vi
TABLE OF CONTENTS .....	vii
LIST OF FIGURES .....	viii
LIST OF TABLES .....	x
1. INTRODUCTION AND STATEMENT OF THE PROBLEM .....	1
2. BACKGROUND INFORMATION .....	3
2.1 Radiation Detection .....	3
2.2 Detector Design .....	5
2.3 Bordon Carbide, B <sub>4</sub> C .....	14
2.4 Sources of Signal Noise .....	16
2.4.1 Electronic Sources of Noise .....	17
2.4.2 Mechanisms for Microphonic Sensitivity .....	22
3. MATERIALS AND METHODS .....	24
3.1 Equipment Description .....	24
3.2 Preliminary Investigation & Sensitivity Analysis .....	25
3.3 Microphonic Noise Testing .....	26
3.4 Neutron Counting .....	29
4. RESULTS AND ANALYSIS .....	32
5. CONCLUSIONS AND FUTURE WORK .....	39
REFERENCES .....	41

## LIST OF FIGURES

	Page
Figure 2-1. Pulse height spectrum of boron-lined detector .....	5
Figure 2-2. Section view of the detector .....	7
Figure 2-3. Expanded section view of the detector .....	8
Figure 2-4. Cutaway view of the detector .....	10
Figure 2-5. Section view of the detector .....	12
Figure 2-6. Electrical connections of the detector.....	13
Figure 2-7. Block diagram of the detector system .....	13
Figure 2-8. Example of electrical noise .....	17
Figure 2-9. Example of electrical noise from outlets .....	18
Figure 2-10. Example of electrical noise from light ballasts .....	18
Figure 2-11. Before image of electrical connections .....	19
Figure 2-12. After image of electrical connections.....	20
Figure 2-13. Before image of the top of aluminum foil shielding .....	21
Figure 2-14. Before image of the bottom of aluminum foil shielding .....	21
Figure 2-15. After image of steel shielding.....	22
Figure 3-1. Example of a neutron count.....	27
Figure 3-2. Experimental set-up to obtain neutron count.....	30
Figure 3-3. Experimental set-up to obtain neutron spectrum.....	31
Figure 4-1. Bias voltage impact on detector's response to sound.....	33
Figure 4-2. Detector response to sound at 0 bias voltage.....	34

	Page
Figure 4-3. Before image on cables response to sound.....	35
Figure 4-4. After image on cables response to sound .....	36
Figure 4-5. Detector response to sound at 0 bias voltage after cable replacement .....	37
Figure 4-6. Pulse height spectrum with detector.....	38

## LIST OF TABLES

	Page
Table 3-1. The equipment list and model numbers are shown below.....	25

## 1. INTRODUCTION AND STATEMENT OF THE PROBLEM

Computational models are used extensively in reactor designs (NRC 2015). Any improvement on the physics and computational models used, whether optimizing for parallelizability or creating a more accurate or robust model, will improve reactor designs in the future. New models inherently need experimental measurements for validation. Neutron fluence measurement in a highly variable gamma and neutron field under changing reactor conditions present significant engineering challenges for detector design. This project focuses on resolving most of those challenges.

In a nuclear reactor, there are instrumentation channels in the fuel assembly that are used for recording neutron fluence or temperature. Measurements with these detection systems help to effectively characterize the reactor operations. The 1 MW Training, Research, Isotopes, General Atomics (TRIGA) reactor located at the Nuclear Science Center in College Station, Texas, is no different (Newhouse 2015). Regretfully, the location of the current instrumentation is inadequate to validate new calculations of the reactor's transient response (Adams 2012). To provide experimental validation of the calculations, a new detection system was designed to collect data from locations between the fuel rods. This data could then be used to validate the computational model for neutron transport.

In order to fit between the fuel rods, the outer diameter of the detector assembly is constrained to less than 19 mm. After an experimental safety analysis, the design was further constrained to have an outer diameter of 11 mm. This was to ensure safety

margins for coolant flow and minimal perturbations to the reactor's environment. Because of the potential radiation damage to plastic insulators, the coaxial cables to the detector had to end at least 50 cm from the center of the core. The design selected utilized a 90 cm long rigid coaxial structure with a 2 cm long, 5 mm diameter ion chamber at one end and coaxial cable connections for signal and high voltage at the other end. During preliminary testing of the partially constructed detector, it was found to have extreme microphonic sensitivity to normal sound levels in addition to electronic noise. For example, talking in the same room as the detector would create a signal larger than the expected electrical pulse from a neutron measurement.

The subject of this study is the testing of the partially constructed neutron detector and determination of design features to minimize microphonic noise. Included in this report are recommendations for future detector design.

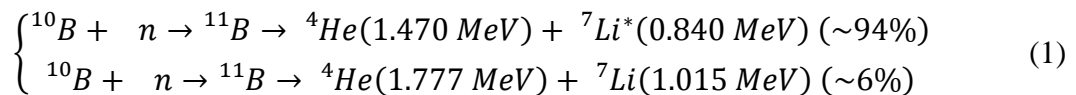
## 2. BACKGROUND INFORMATION

### 2.1 RADIATION DETECTION

Physical processes that transfer energy through space without the need for a transfer medium are known collectively as “radiation.” Specifically, ionizing radiation transfers sufficient energy to ionize atoms and molecules. Ionizing radiation can take the form of charged or uncharged particles or photons. Uncharged particles, like neutrons, present significant challenges for measurement, therefore it is typical to measure the charged particles after a neutron interacts. The neutron capture in  $^{10}\text{B}$  was chosen as the best method to convert thermal neutrons to easily measurable charged particles. Measurement of thermal neutron flux as a function of time is an appropriate way to validate the transient reactor calculations.

The interaction probability of neutrons with  $^{10}\text{B}$  is a function of the neutron’s energy. The term used to describe this probability of interaction is the microscopic cross-section, in units of barns. The cross section of  $^{10}\text{B}$  capture for a 2 MeV neutron and release of an alpha particle is 2.068 barns, but for a thermal neutron (0.025 eV) the cross-section is 3870 barns (Hale 2012).

When  $^{10}\text{B}$  absorbs a neutron, it becomes  $^{11}\text{B}$ , which then quickly decays by alpha emission to  $^7\text{Li}$  as shown in equation 1. The more likely reaction has the  $^7\text{Li}$  in an excited state (Siciliano 2012).



From conservation of momentum the helium and lithium particles are emitted in opposite directions. In boron lined detectors only one of the two products can travel through the detection volume and ionize the gas. The other product's energy would be lost within the wall of the detector.

The products of the  $^{10}\text{B}(n,\alpha)$  reaction then ionizes gas in the detection volume, separating the electrons from the gas atoms. The positively charged gas ions are collected at the wall and the electrons are collected on the center electrode with the center electrode being at a positive bias relative to the wall. The voltage can be reversed in polarity for the opposite charge to be collected on the anode. If the detector size is small (as it is in this case) not all of the energy from one of the product, will be transferred to gas ions and electrons before it collides with the opposite wall of the detector. Likewise, if the detector volume is large, such that all of the energy from the ionizing trail by the charged particle could be collected, we would expect a spectrum as shown in Fig. 2-1 for a similar detector tested by Pacific Northwest National Laboratory (Siciliano 2012). PNNL's boron lined detector was 2.54 cm in diameter. The maximum energies for  $^4\text{He}$  (1.470 MeV) and  $^7\text{Li}$  (0.840 MeV) causes the two sharp drops in the spectrum. Since charged particles produced inside the boron layer deposit part of their energy before entering the gas, they produce a nearly constant number of events with energy from the maximum to zero. While both  $^4\text{He}$  and  $^7\text{Li}$  are equally likely to be measured in a large detection volume, the number of lower energy events of  $^4\text{He}$  add to the counts for  $^7\text{Li}$ , hence the double plateau shown in Fig. 2-1.

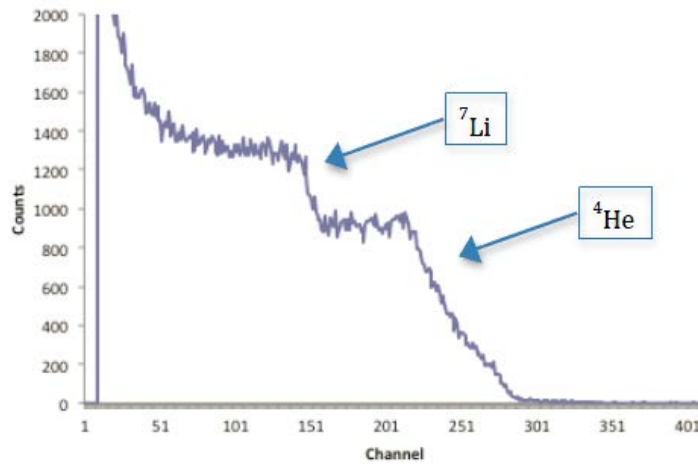


**Figure 2-1.** Pulse height spectrum for their 2.54 cm diameter boron-lined detector (Siciliano 2012).

The total charge,  $Q$ , is the sum of the charge of all of the electrons liberated during the interaction event, results in the current pulse sent through the anode wire. The current is sent to a charge sensitive pre-amplifier that produces a voltage step,  $\Delta V$ , proportional to the collected charge. The shaping amplifier then takes the voltage step and forms it into a suitable pulse for detection. Care must be taken to minimize pulse-pile up and electronic noise while ensuring that enough meaningful signal is collected by careful selection of the shaping time (Knoll 2010).

## 2.2 DETECTOR DESIGN

As stated previously, the current instrumentation location inside the 1 MW TRIGA reactor core at the Nuclear Science Center was insufficient to validate new calculations of the reactor's transient response during pulse operation. To provide experimental validation of the calculations, a new detection system was designed to measure thermal neutrons from different positions inside the core and between the fuel rods themselves.

The data collection requirements drove the initial parameters for the design, specifically the external diameter of the detection system, and a maximum allowable size and height of the active volume to ensure that the detector approximated a point in the reactor. The external diameter was initially constrained to less than 19 mm, which was later reduced to 11 mm to ensure adequate coolant flow. The height of the active volume of 2 cm was found to be appropriate for approximating a point detector. Figure 2-2 shows both the 19 mm external diameter at the top of the detector structure and the 11 mm reduction at the bottom to minimize the reduction of the coolant flow that the detector would cause in the core of the reactor.

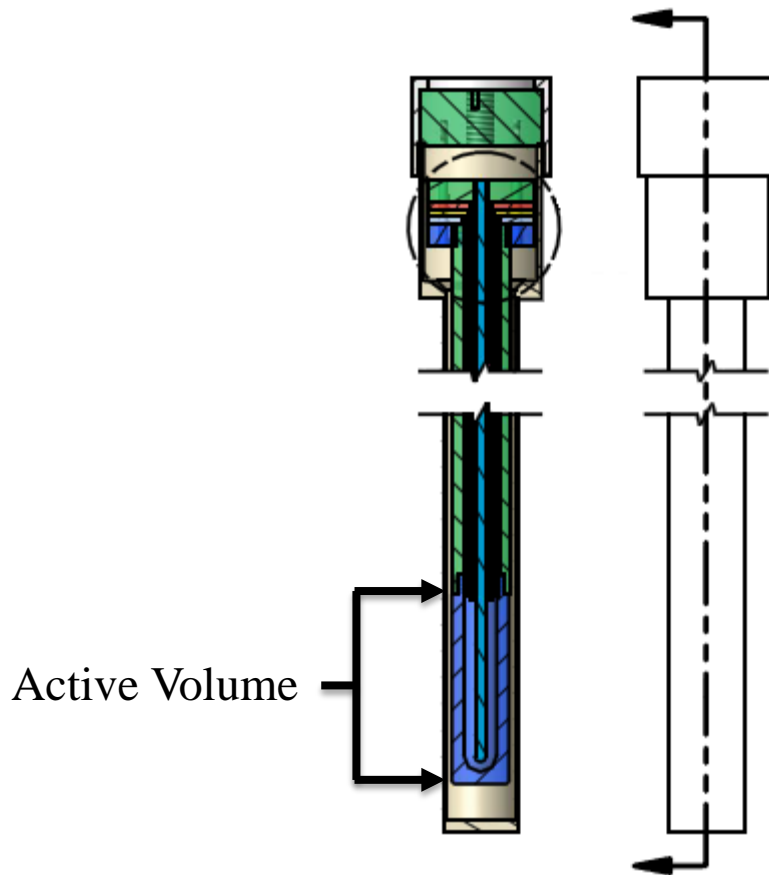


**Figure 2-2.** The section view of the detector shows the active volume at the bottom, and several concentric tubes of aluminum and glass which are adhered to plastic washers (circled area) for support. An expanded view of the plastic washers is shown in Fig. 2-3.

The potential for radiation damage to plastic washers and coaxial cables resulted in all plastic components being placed at the opposite end from the active volume. A minimum distance of 50 cm from the center of the core was needed to minimize damage to the plastic washers and coaxial cables, which then led to the detectors total length becoming 1 m. This length ensured that, at the lowest location for data collection in the

core, the plastic remained approximately 50 cm away from the center of the core. This also ensured that the detector would have reusable cables and connectors. Aluminum was chosen for the tube design for its low absorption cross section, which minimized activation. Figure 2-3 expands on the plastic washers located at the top of the detector, which the aluminum tubes and glass tubes were connected to.

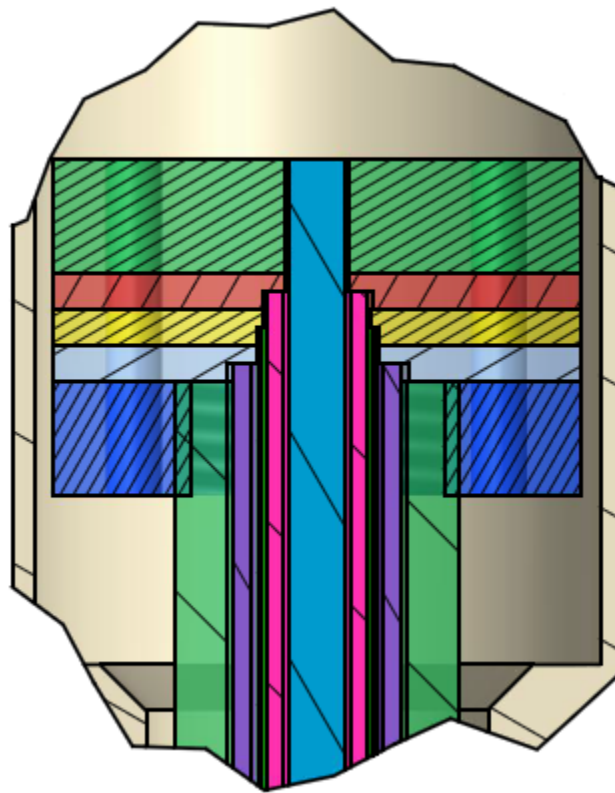


**Figure 2-3.** The expanded section view of the detector shows the plastic (salmon and light blue) and metal washers (green, yellow, and dark blue), along with the concentric tubes of metal and glass. The washers and various tubes would be supported by threaded studs extending from the top cap of the outer aluminum tube.

Two MICRODOT® connectors at the top of the detector would handle detector bias voltage and signal. Cables from the MICRODOT® connectors would then interface with a Data Acquisition System (DAQ) for collection and post processing.

A three component, grounded aluminum shield minimized interference from electronic noise. The first of the three parts was the 1 m long tube that would house the internal components of the detector. The bottom of the tube was sealed with an aluminum plug and the top was threaded. The next component was the cylindrical disc that the two MICRODOT® connectors, vacuum line, and studs supporting internal components were attached to. This cylindrical disc was then tightly sealed with a threaded aluminum cap. This cylindrical disc, or vacuum chamber base, would provide the electrical interface between the internal and external components of the detector. The tightness of the seal between the cylindrical disc and the 1 m long tube was ensured by using an indium wire gasket. Different alloys of aluminum were used to prevent galling. The MICRODOT® connectors and vacuum line copper tube were sealed around the edges with Torr Seal®. The external diameter of the top of this 1 m long detector was 19 mm while the external diameter 31 mm from the top was reduced to a diameter of 11 mm. This reduction ensured adequate coolant flow between the fuel rods of the nuclear reactor. These dimensional requirements led to extremely tight tolerances of five-thousandth of an inch ( $\pm 0.127$  mm) which led to complications with material selection, construction, and assembly.

The next driving element of the design was the active volume for thermal neutron detection. The subject of this study uses a boron carbide lining with a thickness of 1.4

$\mu\text{m}$  inside a 2 cm length thin copper straw with a diameter of 4.60 mm. The enrichment of  $^{10}\text{B}$  was 96.55 atom percent (Proportional Tech. 2015). The copper straw was internally placed within an aluminum head. The aluminum head was threaded on one end, so that the active volume could be replaced at the end of life. The high voltage walls of the detector that the aluminum head screwed into were designed to be insulated from the grounded aluminum tube with plastic fiber. The 870 mm long high voltage tube then screwed into a custom designed brass washer. The brass washer acted as the interface between the high voltage tube and the MICRODOT® connectors. Once the high voltage walls were designed, the anode wire dimension was selected for the uniformity of the electric field in the active volume. The various concentric tubes of metal and glass are shown where they end near the active volume of the detector in Fig. 2-4.

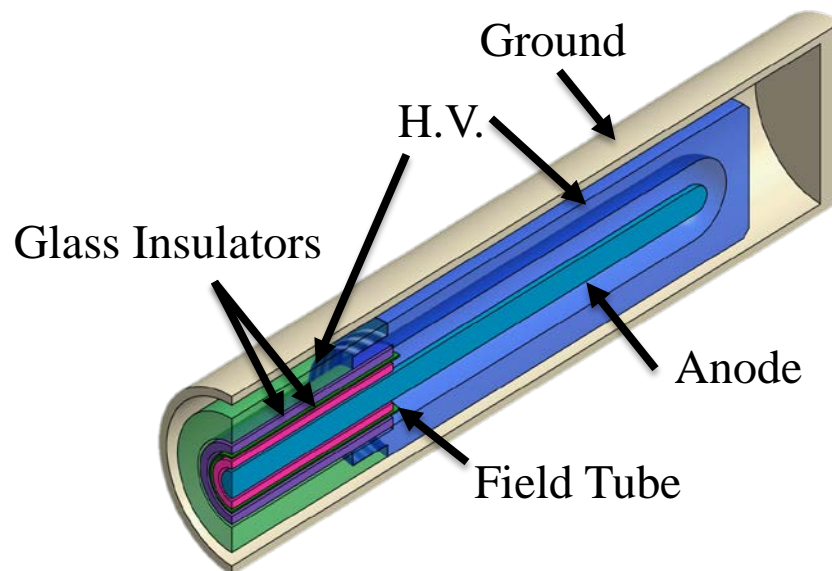


**Figure 2-4.** The cutaway view above shows the ground, H.V., both glass insulators, the field tube, and the anode wire.

While neutron detection can only occur in the active volume, in the presence of a large gamma field the rest of the high voltage tube and anode wire could act as an ion chamber. To prevent charge collection from gamma radiation, the potential charges need to be neutralized before reaching the anode wire. The design included a metal tube (guard tube) between the anode and high voltage tube. To prevent the metal tube from contacting the anode wire or high voltage walls, two insulating glass tubes were selected to surround the anode wire, and fit within the high voltage tube. Brass was selected as the guard tube material instead of a rigid metal tube of aluminum because it was both readily available and conformed to the tight dimensional requirements. The brass strip was wrapped around the inner glass tube. This brass strip is held at essentially the same electric potential as the anode. The resulting lack of electric field strength ensured that charge collection by the anode wire occurred only in the active volume.

The last step of the design was to determine how to securely mount and electrically connect the needed tubes and components to the cylindrical plug. Both the MICRODOT® connectors for high voltage, the signal cable, and a tube for vacuuming and gas placement were housed on the cylindrical plug. Custom made metallic and plastic washers were chosen to secure the metal and glass tubes. Electrical connections between the washers, the anode wire, and high voltage tube were secured by threading both the high voltage tube and the anode wire. The field tube was secured to the washer with conductive silver epoxy. Each of the three washers had electrical wires leading to two MICRODOT® connectors and ground. The glass tubes were secured to the plastic

washers with cyanoacrylic. All five washers were mounted to the vacuum chamber base with plastic 0-80 screws.

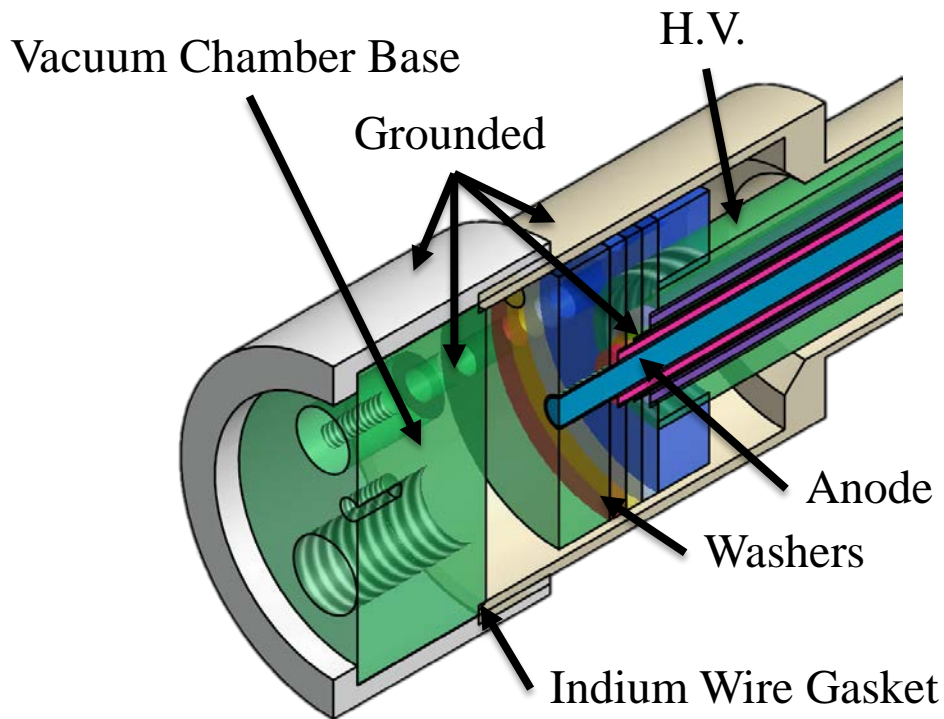


**Figure 2-5.** The section view of top of the detector shows the connections between the anode wire, field tube, glass tubes, and H.V. and their respective washers. Electrical connections would then be made from the washers to the MICRODOT® connectors located on the vacuum chamber base.

The charge was captured with the anode wire in the center of the active volume. The anode signal, which was a measured current pulse, went to a charge sensitive pre-amplifier. The brass wrap, which was the field tube that wrapped around an insulating glass layer, was electrically grounded. The external walls of the detector volume were driven at a negative voltage so that the electrons released from the ionization of the fill

gas would be driven towards the center anode wire for collection. The cutaway view shown in Fig. 2-6 reveals the concentric nature of the design.

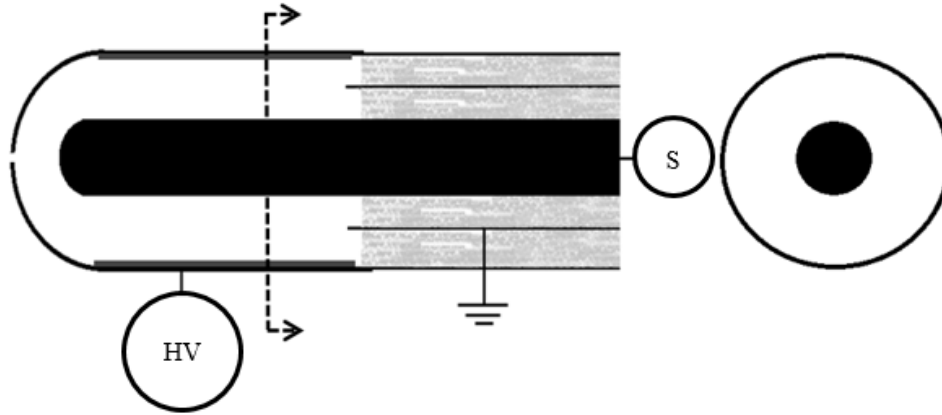


**Figure 2-6.** The anode transmits the current pulse as signal, the walls of the active volume were driven with a bias voltage.

Figure 2-7 shows the block diagram on how the entire system was connected. The signal from the anode wire sends a current pulse into the pre-amplifier. From the pre-amplifier the signal then was sent to a Gaussian shaping amplifier. From the shaping amplifier the signal was split and sent to the oscilloscope and a Multi-Channel Analyzer (MCA) for analysis.

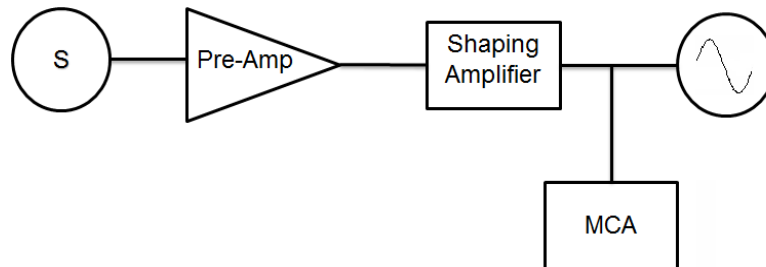


**Figure 2-7.** The block diagram above shows the connections for the oscilloscope and MCA.

The detector was never fully assembled during the testing phase. Evaluating this design at an intermediate stage helped identify and eliminate potential issues without requiring the disassembly of the entire system. Specifically, the electrical shielding of the external aluminum tube, plug, and cap were not used. This in turn, meant that there were no reliable electrical connections.

### **2.3 BORON CARBIDE, B<sub>4</sub>C**

The active volume of the detector uses a 1.4 μm thick layer of 96.55% enriched <sup>10</sup>B deposited with the chemical vapor deposition technique on the inside of a 2 cm long copper straw (Besmann 1988). The length of 2 cm when compared to the height of the reactor at the NSC can be considered a point. The 96.55% <sup>10</sup>B enrichment ensures a high reaction rate of thermal neutrons in the sensitive volume. What follows is the description of what the minimum signal needed for detection is, and thus what an acceptable electrical noise level could be for the detector system.

The minimum path length,  $\mathcal{L}$ , in units of mm for detection depends on the minimum energy,  $E_{min}$ , in units of MeV needed for detection and the Linear Energy Transfer (LET) in units of MeV/mm. Equation 2 can be used to determine if there is sufficient path length for signal measurement.

$$\mathcal{L} = \frac{E_{min}}{LET} \quad (2)$$

The minimum energy for detection depends on the minimum charge,  $Q_{min}$ , in units of Coulombs needed for measurement, the W-Value of the gas in units of

MeV/ion-pair, and Coulomb's constant,  $k$ , which is  $1.6 \cdot 10^{-19}$  C/ion-pair as shown in equation 3.

$$E_{min} = \frac{Q_{min} \cdot W}{k} \quad (3)$$

The minimum charge for detection depended on the minimum detectable pulse height,  $MDPH$ , in mV and the experimentally measured gain,  $G$ , in units of C/mV of the system as shown in equation 4.

$$Q_{min} = MDPH \cdot G \quad (4)$$

The  $MDPH$  depends on the root mean square (RMS) of the system noise,  $Noise Floor$ , in units of mV as measured from the output of the Gaussian shaping amplifier with identical gain settings needed for neutron detection. The constant of 5 ensures that any pulse measured was indeed from a thermal neutron interaction, instead of from random fluctuating noise. Equation 5 shows this relation.

$$MDPH = 5 \cdot Noise Floor \quad (5)$$

Finally the gain of the system,  $G$ , can be determined from multiplying the capacitance of the charge sensitive pre-amplifier,  $C$ , in units of farads with the voltage of the test pulser,  $V_{Pulser}$ , in units of volts needed to create a pulse height of the same magnitude as the measured neutron signal and dividing by the measured maximum voltage of the Gaussian shaping amplifier,  $V_{Amplifier}$ , in units of mV as shown in Equation 6.

$$G = \frac{C \cdot V_{Pulser}}{V_{Amplifier}} \quad (6)$$

The minimum energy needed to overcome the electrical noise is 170 keV. When these calculations are carried out for both the  $^4\text{He}$  and  $^7\text{Li}$  nuclides the minimum path length for detection are found to be 6.7 mm and 4.1 mm respectively. The internal diameter of the copper straw is 4.60 mm. The anode wire has a diameter of 1.58 mm. The minimum air gap between the outer edge of the thick anode wire and the inner wall of the boron carbide coated straw is 1.51 mm. The height however for the boron lined copper straw does provide sufficient length for charge collection.

The absorption cross section of  $^{10}\text{B}$  for thermal neutrons are almost 2000 times more than the absorption of a 2 MeV neutron. From the mass energy conversion and momentum conservation equations, the energy available for the two products are 1.470 MeV for the  $^4\text{He}$  nucleus and 0.840 MeV for the  $^7\text{Li}$  nucleus. Of this available energy, some will be deposited in the 1.4  $\mu\text{m}$  thick boron carbide walls. Using For a helium nucleus of 1.470 MeV, the projected range calculated using the Stopping and Range of Ions in Matter (SRIM) software package is 3.36  $\mu\text{m}$  in  $\text{B}_4\text{C}$ , likewise for a lithium nucleus of 0.840 MeV, the projected range is 1.71  $\mu\text{m}$  (Ziegler 1985). Increasing thicknesses of  $\text{B}_4\text{C}$  would not drastically improve the detectors count rate.

## **2.4 SOURCES OF SIGNAL NOISE**

Early in testing of the partially constructed neutron detector, sensitivity to electrical and audible noise was observed. While almost all of the electronic noise issues were resolved with a redesign of the intermediate electrical connections and electromagnetic shielding, repeated electrical signatures were still observed.

### 2.4.1 Electronic Sources of Noise

At multiple times the ground was accidentally disconnected. Figure 2-8 below shows that repeated shape from the output of the shaping amplifier indicating that the noise was produced by a continuous wave source. If the electrical noise originated from the pre-amplifier there would have been no clear repetition in signal. Noise with a repetitive nature must be driven by an external source and therefore can be eliminated by adequate shielding.



**Figure 2-8.** Repetitive signals of a large magnitude were easily eliminated with improvements in grounding.

Even with ground securely connected, if the temporary electromagnetic shielding was not properly set-up, or if the signal wire was exposed a noise signal with a 16.8 ms period corresponding to a 59.5 Hz electrical signal could be seen as in Fig. 2-9. The 60 Hz signal obviously comes from the frequency that power is delivered from the electrical grid.

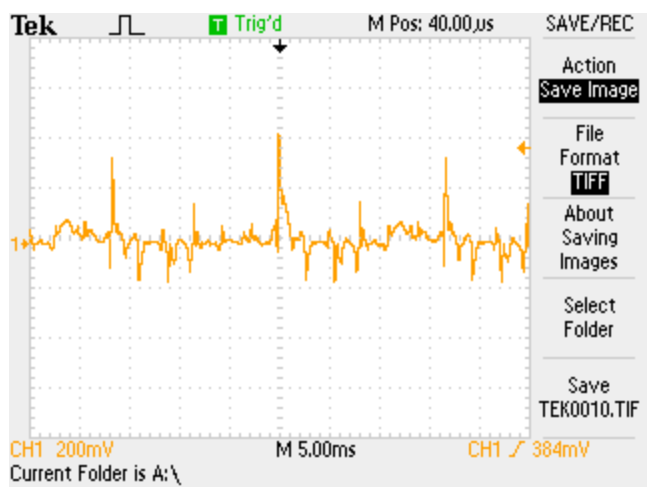


**Figure 2-9.** The current generated in the detector matched the frequency of power found in outlets.

The last easily identifiable repeated electrical signal was the 21  $\mu$ s period or 47.6 kHz electrical signal as shown in Fig. 2-10. When the fluorescent lights in the lab were turned off, this signal went away. Most likely a result of the fluorescent lights' ballast's design, this led to all the experiments being performed with the lights off, to minimize sources of potential noise.

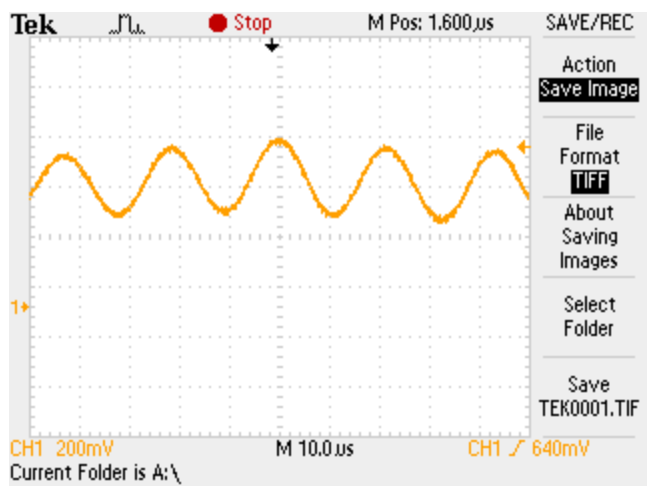


**Figure 2-10.** The 47.6 kHz signal is most likely from light ballasts.

Most of the electrical signals came from poor electrical connections and electromagnetic shielding. Once the electrical connections were redone, the detector was less sensitive to electrical noise.

Most of the electronic sources of noise were easily eliminated with resoldering the loose floating connections to a copper clad perforated board. A comparison of Fig. 2-11 and Fig. 2-12 show a before and after of the soldered connections.

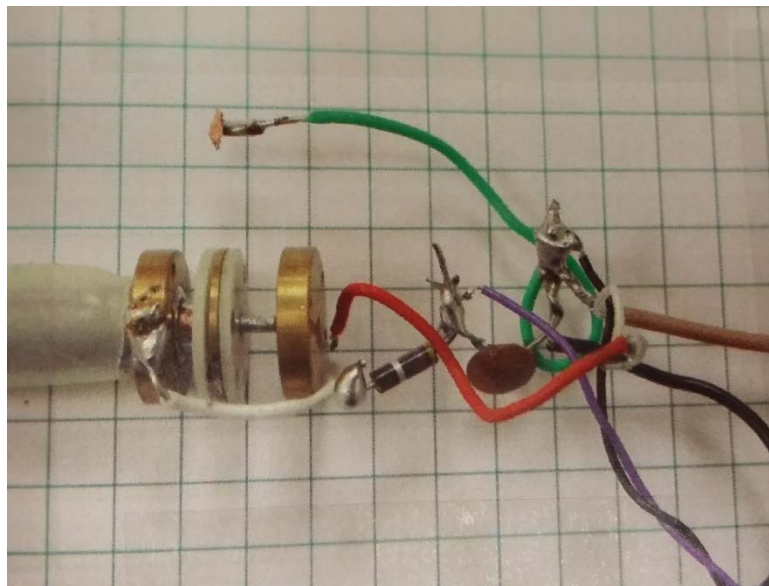


**Figure 2-11.** The original electrical connections were inadequate for repeated testing.

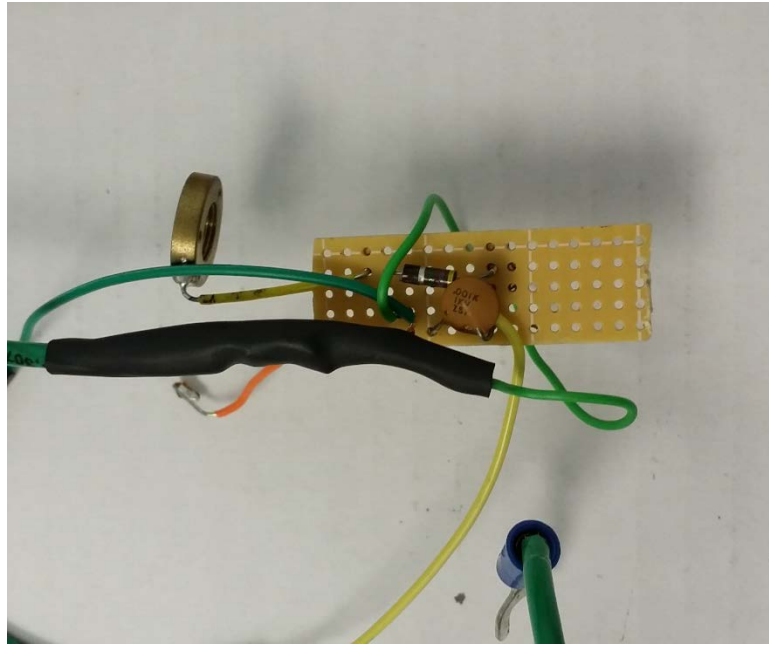


**Figure 2-12.** The improvements of no floating electrical connections, decreased length of wires and improved flexibility reduced the electrical and sound sensitivity.

The rest of the major electronic noise was minimized with the use of a better grounding shield. The original single layer of aluminum foil was found to be inadequate in properly protecting the circuit from the signals present in the lab space. Using a long, thick steel tube minimized the electronic noise. Both Fig. 2-13 and Fig. 2-14 show the initial shielding arrangement with aluminum foil. The improvements to the electrical shielding are shown in Fig. 2-15.

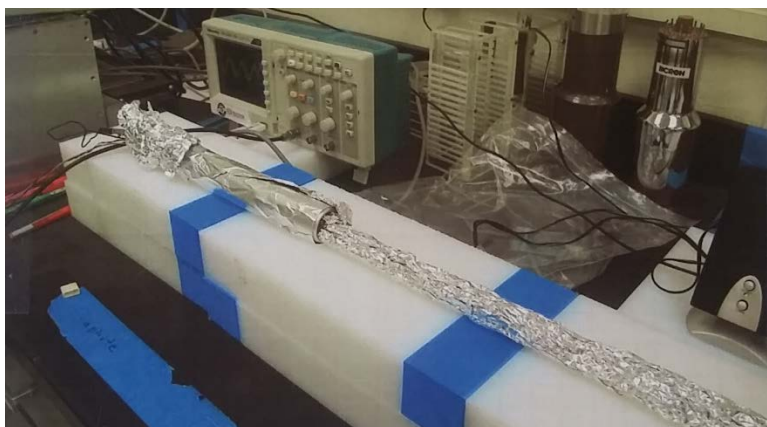


**Figure 2-13.** The top portion with the electrical connections is located within the aluminum foil roll at the top of the detectors.

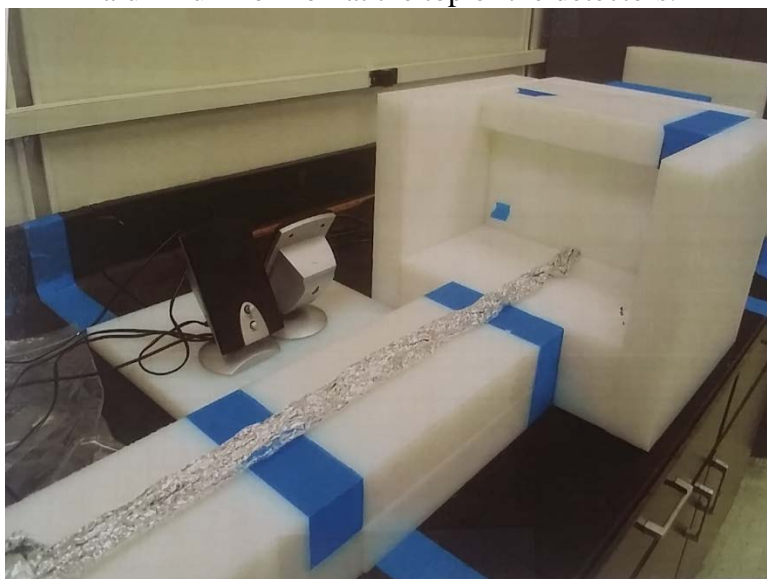


**Figure 2-14.** The bottom portion of the detector where the active volume is located is shown here.

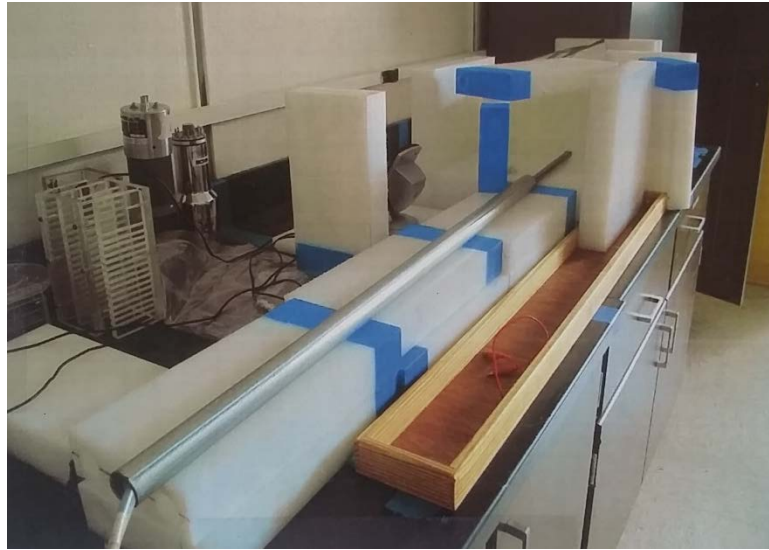


**Figure 2-15.** By using a larger shield, a significant amount of electronic noise was eliminated.

#### *2.4.2 Mechanisms for Microphonic Sensitivity*

With most of the sources for electronic noise understood, various mechanisms for the detector systems sensitivity to audible sound were investigated. Early in testing of the partially constructed detector, repeated waveforms were observed. Some of the waveforms were identified as coming from electronic sources as discussed in the previous section, while other waveforms were isolated as coming from talking in the laboratory. This was an unexpected and surprising revelation. There are a number of potential reasons that this exists, discussed below.

Poor electrical connections between the anode and the charge sensitive pre-amp could mechanically vibrate generating a signal. Because of the tight tolerances it seemed believable that the anode wire vibrating in a high voltage environment could change the capacitance of the system causing a signal. Even in a low to zero voltage environment,

the anode shifting relative to the outer walls could still squeeze the glass acting as a dielectric and change the capacitance which would then generate a signal.

The triboelectric effect is the electrical charging of two dissimilar materials that are mechanically moving against each other, usually in the form of friction. The tight tolerances could lead to this effect. Yet another option was that the charge sensitive pre-amp was sensitive to mechanical vibrations of the voices, and later the speakers used in testing the system. Lastly, the coaxial cable itself could be undergoing a piezoelectric effect generating signal by compression of the dielectric between the anode and the cathode.

### 3. MATERIALS AND METHODS

Three main procedures were performed in the testing the partially constructed detector system. The first preliminary process was assuring that all electrical connections were made, and that the noise level was low enough that neutron detection would be possible. The second procedure related to the actual testing of the systems microphonic sensitivity. Finally, the third procedure was an actual neutron count with the functioning partially constructed detector system. There are several methods to effectively test the partially constructed detector system. The first steps would be to characterize and identify the source of the noise in the detection system. Once the cause was identified, the next step was to develop an effective testing regime to evaluate the magnitude of the noise's impact on the detector system.

#### **3.1 EQUIPMENT DESCRIPTION**

As with most detector systems, a detector was connected to a charged sensitive pre-amplifier. The output of the pre-amplifier was then connected to the Gaussian shaping amplifier in a Nuclear Instrumentation Module Bin (NIM Bin). From the output of the shaping amplifier a tee connector would split the signal to an oscilloscope and true RMS meter for analysis. The NIM Bin is based on the DOE/ER-0457T standard.

**Table 3-1.** The equipment list and model numbers are shown below.

Equipment	Model & Serial Number
NIM Bin	Ortec, Model 401A and Model 402A Power Supply
HV Supply	ORTEC Model 428 Detector Bias Supply
Pre-Amplifier	Canberra 2006 Serial # 12072801
Test Pulser	ORTEC Model 480 Serial # 1819 Rev. 28
Shaping Amplifier	ORTEC Model 570 low gain Serial # 07130593 Rev. Y
Oscilloscope	Tektronix Serial # TDS1002C-EDU, C011809
True RMS Meter	FLUKE 45 Dual Display Multimeter, Serial # 5520016

### **3.2 PRELIMINARY INVESTIGATION & SENSITIVITY ANALYSIS**

When the detector was initially studied, the electronic noise was such that a test pulser signal would be unidentifiable. After careful resoldering of the electrical connections, and trimming the excess length of the leads, only some of the noise dissipated. Since this detector system was never fully constructed, there were no cables with MICRODOT® connectors at the end of the detector system, nor were there a solid electrical shield surrounding the system.

Heat shrink tubing was used to separate the HV from the grounding system used for this detector. Originally, the grounding system or electrical shield was aluminum foil wrapped around the aforementioned heat shrink tubing. While this did reduce the electrical noise, certain repetitive wave forms were observable in the output of the Gaussian shaping amplifier. This eventually led to the conclusion that a steel tube of sufficient length to enclose the detector system would decrease the electrical noise further, which it did. Having reduced the electrical noise to a point that the test pulser

signal of 6.32 mV was now identifiable an experimental procedure for quantifying the microphonics noise was the next priority.

A preliminary frequency sensitivity analysis at a constant detector bias voltage revealed that the detectors response to sound could be evaluated at 10 Hz intervals from 100 Hz to 2000 Hz. The 10 Hz increment was later increased to 50 Hz, since no peaks in response were detected at 10 Hz increments and an experiment could be repeated five times with the 50 Hz interval in the time required for a single experiment with 10 Hz increments.

Finally the sensitivity to bias voltage was determined. The bias voltage was set to a specific value, after 1 minute of settling time, a frequency response sequence was run. The voltage was then increased in 50 V increments and the frequency response sequence was run again. The sensitivity analysis performed was essential in providing meaningful insight into the detectors systems response while minimizing tedious or inconsequential parameterization or data collection.

### **3.3 MICROPHONIC NOISE TESTING**

The detector's sensitivity to sound could be a result of numerous scenarios. Effective characterization of this phenomenon was needed to accurately determine if the sensitivity to noise was consistent and repeatable, and to determine how mechanical and electrical variables impacted the sensitivity. Since the magnitude of the sensitivity would obviously be changed by the settings of the Gaussian shaping amplifier, the first step was to determine what gain was needed for neutron detection.

A testing environment was created to determine the gain needed to detect a neutron signal. An ideal testing environment being defined as no appreciable electronic noise as seen on the shaping amplifier output to the oscilloscope and acoustically quiet. Initially a neutron source,  $^{252}\text{Cf}$ , was placed inside a polyethylene moderator to create thermal neutrons. Figure 3-1 shows a typical thermal neutron count. This initial detection of neutrons was essential in assuring that the test set-up was adequate to properly study the detectors acoustic response.

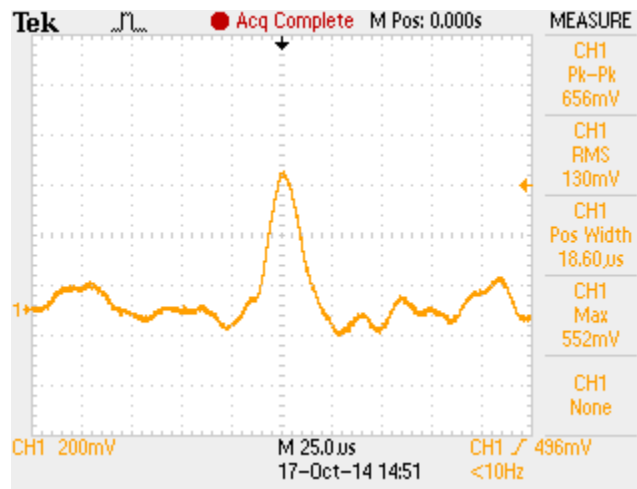


**Figure 3-1.** This neutron count shown is from the output of the Gaussian shaping amplifier with 10  $\mu\text{s}$  shaping time.

Once the gain and voltage settings necessary to detect thermal neutrons were determined, the neutron source was removed, and the settings recorded. A test pulser was also used to artificially recreate a pulse of the same magnitude as that produced by a neutron event. This allowed for quick testing of the entire system to verify that a neutron signal could be detectable.

Having found the settings needed to detect a neutron in an ideal laboratory environment, the testing commenced. The output of the Gaussian shaping amplifier was monitored with a true RMS voltmeter. The sinusoidal tone was generated with a computer program ToneGen Version 1.04 (Scanlon 2013). Two external speakers were securely attached to the wooden platform in a repeatable configuration with the volume set to maximum. The volume within the program was always set to maximum, while audio output level of the computer that the software was installed on was always set to 50%. This was done so that at maximum response there would be minimal clipping on the oscilloscope used to verify ambient and transient conditions. This also allowed for repeatable magnitude of volume settings, since neither the software nor the speakers had a reliable way of certifying what volume setting they were at.

The frequency of the sound was changed from 100 Hz to 2,000 Hz at 50 Hz increments. The frequency stability was determined by examining the wavelength from the output of the shaping amplifier with an oscilloscope. A baseline measurement with the minimal ambient noise and a muted audio system was considered 0 Hz for all tests. The frequency response of the detector system was then used as a tool to evaluate how changes made to the detector effected its microphonic sensitivity.

The shielding for the detector system was securely mounted to the wooden platform with adhesive tape. The platform was positioned parallel with ground. For all experiments the detector system was placed in a consistent location and position inside the shielding tube. The coaxial cables were attached to a strain relief to prevent detector movement. Care was taken to ensure proper grounding and shielding from potential

sources of electronic noise. The objective of microphonic testing was to determine what frequencies generated the largest response in the detector system.

Every test run started with a system check. The system check was designed to verify that ground was indeed properly connected, that the system was properly shielded from electromagnetics and that the sound itself would be the largest contributor of signal. The test pulser was used to verify that a neutron signal was indeed detectable if a source was present before microphonic testing took place. A complete test run included five sets of data taken (scans from 100 Hz to 2000 Hz) during the same testing session.

### **3.4 NEUTRON COUNTING**

Once the microphonic noise sensitivity was eliminated neutron response data was collected in an ideal laboratory environment. The specific goal of the neutron measurement was to observe peaks corresponding to the stopping power of  $^4\text{He}$  and  $^7\text{Li}$  fragments from the short lived  $^{11}\text{B}$  nuclide. For real world systems however, some of the energy from the  $^4\text{He}$  peak at 1.47 MeV and  $^7\text{Li}$  peak at 0.840 MeV would be lost transporting through the 1.4  $\mu\text{m}$  boron carbide layer. The stopping power for  $^4\text{He}$  and  $^7\text{Li}$  are 0.26 keV/ $\mu\text{m}$  and 0.43 keV/ $\mu\text{m}$  respectively for air at standard temperature and pressure (STP). The small size of the detector means that neither energy peak should be easily resolved since neither ions would actually deposit their total energy in the volume for the most likely paths that the ions would travel. Two neutron measurements were performed: a preliminary measurement to verify that neutrons were indeed detectable in an ideal environment, and a spectrum measurement performed at the NSC.

As mentioned in section 3.3 Microphonic Noise Testing, for the preliminary measurement, a 0.511 mCi  $^{252}\text{Cf}$  Source was placed in close proximity to the detector with thermalizing slabs of polyethylene plastic surrounding both the source and the detector. While the cause of the microphonic noise was not yet determined, in ideal settings the system was able to effectively detect neutrons.

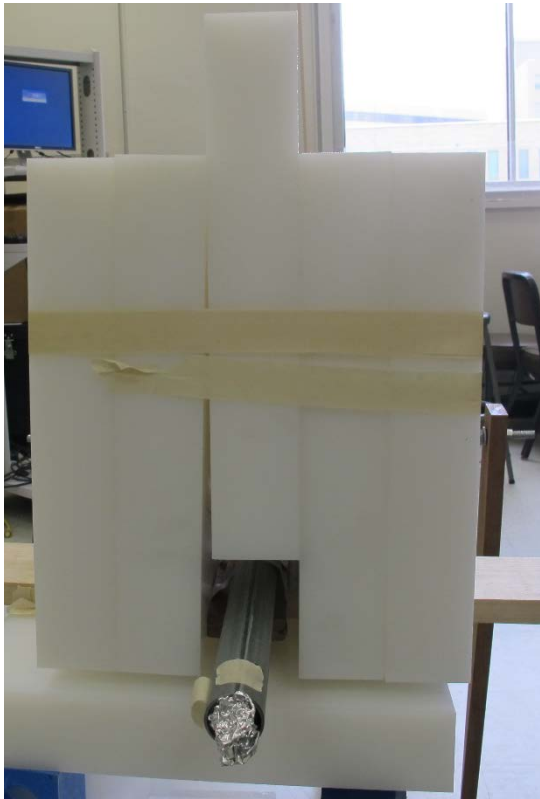


**Figure 3-2.** A  $^{252}\text{Cf}$  neutron source was placed next to the active volume of the detector outside of the electrical shield and surrounded with the polyethylene thermalizing agent.

For the spectrum measurement, the detector system was set to 500 V bias. While neutrons were observed as low as 100 V in the preliminary measurement, 500 V was to assure good ion collection. Within the lower research levels of the NSC, A 2.52 Curie  $^{241}\text{AmBe}$  Source was placed inside a cylindrical polyethylene moderator to produce

thermal neutrons for detection. The detector was set up for a preliminary 20 hour count, followed by a 72 hours count. Finally a background count of the system was also performed for 20 hours in order to be able to subtract remaining noise from the measured spectrum. Figure 3-3 shows the detector system as it was used for the final measurement.

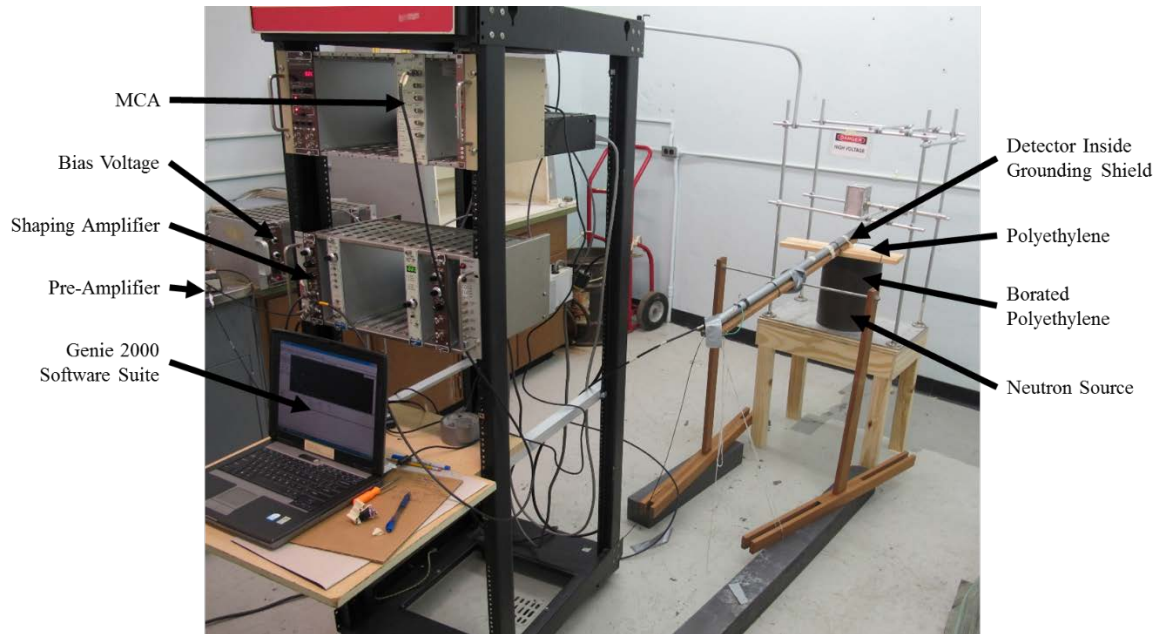


**Figure 3-3.** The neutron source was located at the bottom of a through hole cavity in the center of a cylinder of polyethylene surrounded with brown borated polyethylene for safety.

Data collection was completed with an MCA using Genie 2000 software suite version 3.1. The lower level discriminator was adjusted so that dead time was kept below 10%.

#### 4. RESULTS AND ANALYSIS

The experiments were carried out in three segments as described in the Materials and Methods section. The preliminary investigation was essential in verifying that the thermal neutron signals could be reliably measured and in revealing the correct gain settings used for the microphonic testing and the final neutron counts. Once the preliminary study was performed the detector was evaluated for microphonic sensitivity. Finally after the cause of the sensitivity was eliminated a neutron count was performed.

The experimental design called for bias voltage and output frequency to be varied while the signal response was recorded. Once the sensitivity of the system to perturbation was understood, a more pragmatic testing regime was developed. While evaluating the detector bias voltage, it was found to have no significant impact on microphonic sensitivity, shown by Fig. 4-1. It had initially been proposed that the anode's mechanical vibration results in varying chamber capacitance and therefore varying charge. The charge sensitive preamplifier would provide this charge and produce an output voltage proportional to the charge received or supplied. The bias voltage of the detector did not impact the magnitude of the frequency response, it was easily eliminated from the testing regime. This also meant that the vibrating free end of the anode wire was not the source of the microphonic sensitivity.

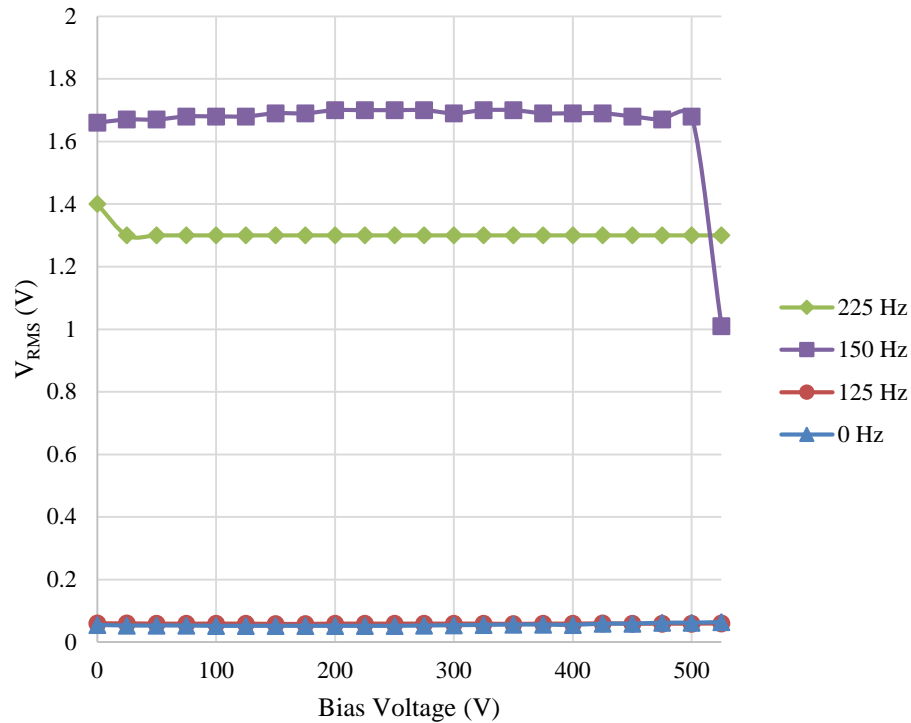


**Figure 4-1.** The bias voltage did not significantly impact the detectors response to sound.

System noise was independent of bias voltage. The system noise was dependent on the frequency. From previous experience a frequency increment of a 100 Hz was large enough to skip over points of interest. An increment of 10 Hz did not contribute significant new insight into a point of interest. The step of 50 Hz intervals was chosen as a tradeoff between meaningful data and rapid collection time.

Once it was realized that the nature of the microphonic sensitivity was not vibration driven change in chamber capacitance, a series of tests were conducted to systematically determine the cause. While some of these possibilities were remote, they could be ruled out by simple experiment. Figure 4-2 shows the RMS of the voltage from

the amplifier while a specific frequency was being tested. In general, the frequency of 450 Hz gave the largest response.

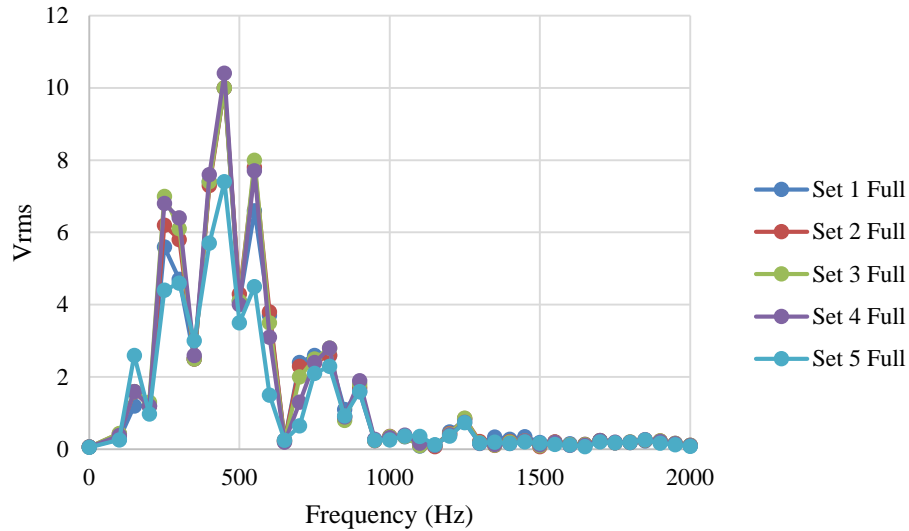


**Figure 4-2.** A typical detector response at 0 V bias.

Possible hypotheses for noise sensitivity, such as vibrations directly causing the preamplifier to generate spurious emissions, were tested and evaluated. Eventually it was determined that the anode cable itself was the sensitive component to the tested audible frequencies. The coaxial cables, two 12' long LMR-240UF, with foam polyethylene dielectric were used for HV and signal connection.

Figure 4-3 shows the frequency response when the cable was mechanically connected to a large metallic rod, of the same approximate length as the detector, insulated inside the electrical shield used in previous experiments but eliminating all detector components. Since the signal had similar peaks between Fig. 4.2 and Fig. 4.3

this is conclusive evidence that a triboelectric or piezoelectric effect in the cable was the source of most of the microphonic noise.

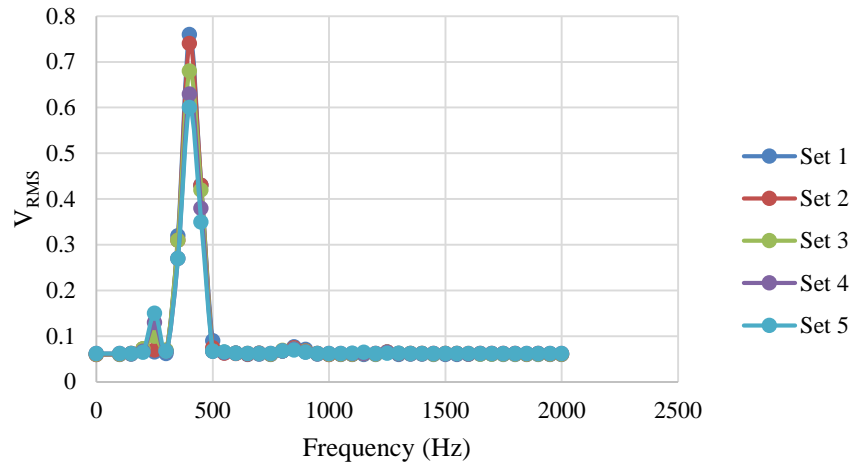


**Figure 4-3.** The magnitude of the electronic noise was essentially unchanged by replacing the ion chamber with a solid steel rod.

The signal cable was replaced with the Super low-noise coaxial accelerometer cable, AO-0038, from Brüel & Kjaer. The frequency response of the replacement signal cable is shown with Fig. 4-4. Both Fig. 4-3 and Fig. 4-4 were performed under similar conditions, but the magnitude of the noise was reduced by more than a factor of 10. The new noise floor for the system was 2 mVAC instead of the 7 mVAC because of the signal cable replacement.

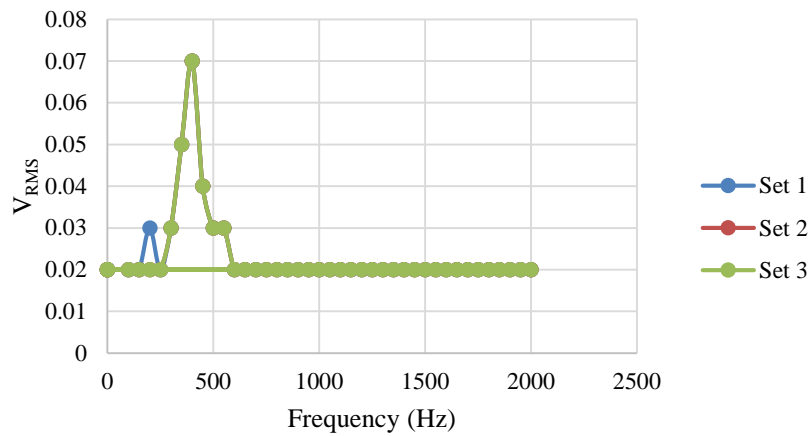


**Figure 4-4.** The magnitude of the electronic noise was reduced by a factor of 10 with the accelerometer cable than with the previous cable.

The large steel rod was removed and the detector components were reconnected. Once the components were reconnected the detectors response to frequency was measured and recorded. The test was performed with the speakers attached in an identical manner, and the sound intensity the same as used in all previous experiments. Figure 4-5 shows the improved response of nearly a factor of 1000.

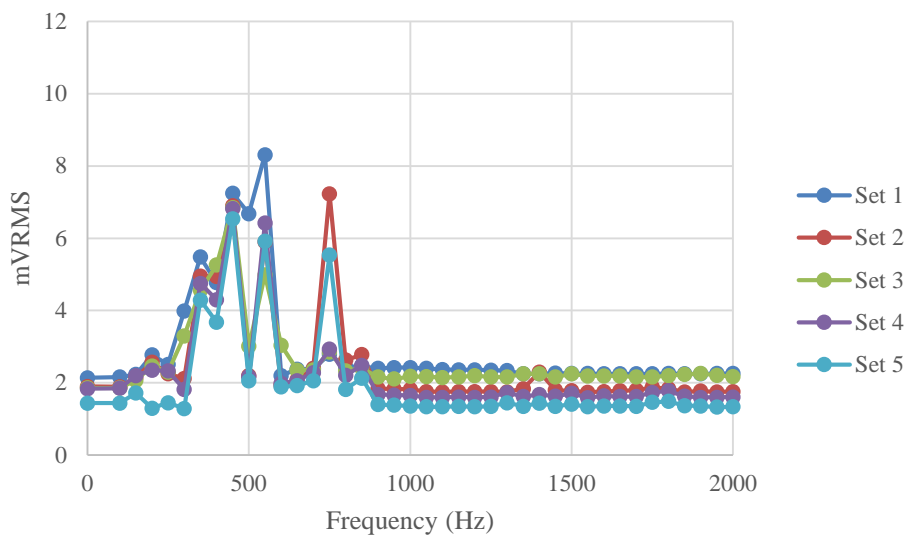


**Figure 4-5.** The magnitude of the electronic noise was reduced by a factor of 1000 with the accelerometer cable than with the previous cable.

With the noise sensitivity nearly eliminated, complete neutron collection could now occur. Figure 4-6 shows preliminary data from a 20 hour neutron count. The black circle indicate an observed wall effect for  $^7\text{Li}$ . It is expected that a longer count would show two distinct wall effects, however only one was observable after 20 hours of counting. However, if the path the ions traveled is too short then we would only expect a single ridge no matter how long a measurement was performed.

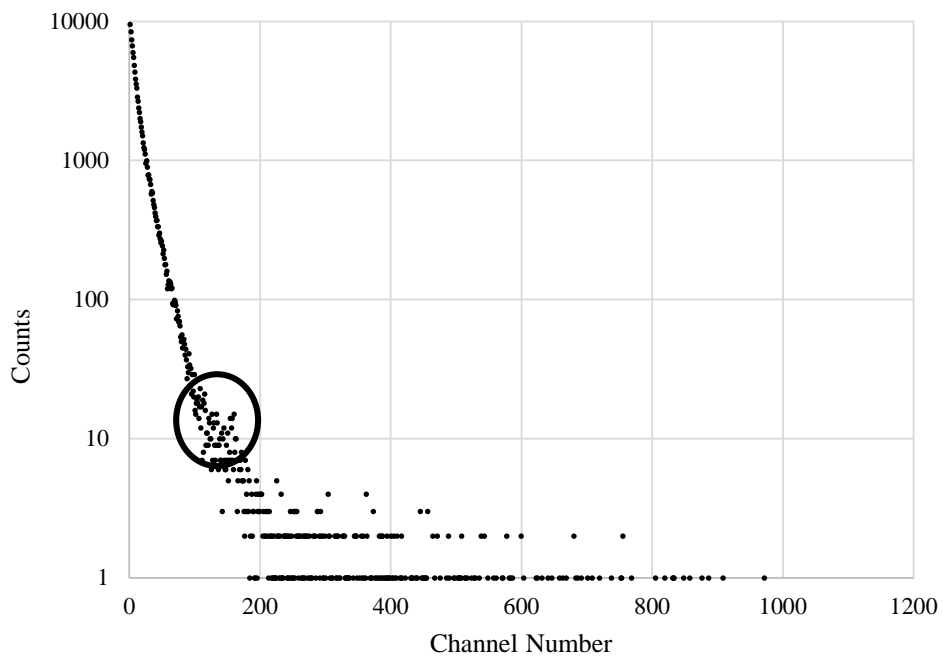


**Figure 4-6.** Pulse height spectrum with log of counts on the abscissa and channel number on the ordinate showing the results for a 4.6 mm diameter boron-lined counter.

## 5. CONCLUSIONS AND FUTURE WORK

The experimental validation of increasingly complex computational models is essential for the design of robust codes. It is only with careful experimental design that meaningful measurements and conclusions can be drawn.

In evaluating possible causes for the initial poor performance of the detector system, it had to be completely disassembled and rebuilt multiple times. The tight tolerances and lack of an electrical connector resulted in the cable being de-soldered and re-soldered every time a test took place. Experimental techniques were improved iteratively. While initial data collection took 3 hours for a complete run, after a sensitivity analysis was performed the time was reduced to 1 hour. Experiments were performed in increasing order of irreversibility of changes in the detector.

Proper construction of the grounding shield would have eliminated initial difficulties with the electronic noise, along with cable connections for this partially constructed detector system. The main issues experienced with the detector system stemmed from its construction and signal cable selection. Throughout the cable construction and selection process, the primary objective was to have the cable connected as close as possible to the anode of the detector system. This minimized the length of the inner conductor in the coaxial cable that was exposed past the cables shielding. The cable was naively selected without consideration for the triboelectric effect. Replacing the cable with a new low-noise cable resolved the microphonic issues and allowed for robust accounting to be performed.

Significant design challenges were resolved that had initially prevented thermal neutron data collection. The sensitivity to electrical noise was mainly a result of poor electrical connections and shielding. When making decisions about an experimental design concise goals and objectives can shorten testing time while yielding desired results. Future work that can be done with this and similar detector systems would include increasing count time to resolve the effects of the wall on the detector system, development of stronger connectors between the washers and their respective rods, and assembling the grounding shield.

## REFERENCES

Adams ML, Higdon DM, Berger JO, Bingham D, Chen W, Ghanem R, Ghattas O, Meza J, Michielssen E, Nair VN, Nakhleh CW, Nychka D, Pollock SM, Stone HA, Wilson AG, Zika MR. Assessing the reliability of complex models : Mathematical and statistical foundations of verification, validation, and uncertainty quantification, Washington, D.C.: Washington, D.C. : National Academies Press; 2012.

Besmann T, Stinton D, Lowden R. Chemical Vapor Deposition Techniques. MRS Bull 13:45-50; 1988.

Hale GM, Young PG. Calculation of Cross Section for a Single Energy [online]. Available at: <http://www.nndc.bnl.gov/exfor/servlet/E4sGetTabSect?sum=1&SectID=334485&req=201>. Accessed 25 Mar. 2015.

Knoll GF. Radiation detection and measurement, Hoboken, N.J.: Hoboken, N.J. : John Wiley; 2010.

Newhouse J. The Texas Engineering Experiment Station (TEES), Texas A&M University System, Nuclear Science Center (NSC) Facility Operating License No. R-83 Technical Specification, "Maximum Power Level":C(1); 2015.

Nuclear Regulatory Commission (NRC). Computer Codes [online]. Available at: <http://www.nrc.gov/about-nrc/regulatory/research/safetycodes.html>. Accessed 25 Mar. 2015.

Proportional Technologies I. Neutron Detection [online]. Available at: [http://www.proportionaltech.com/new\\_site](http://www.proportionaltech.com/new_site). Accessed 26 Mar. 2015.

Scanlon S. Tone Generator 1.04; 2013.

Siciliano ER, Kouzes RT. Boron- 10 Lined Proportional Counter Wall Effects - PNNL-21368; 2012.

Ziegler JF, Biersack JP, Paul H, Webb R, Yu X. The Stopping and Range of Ions in Matter SRIM-2013.00; 2013.